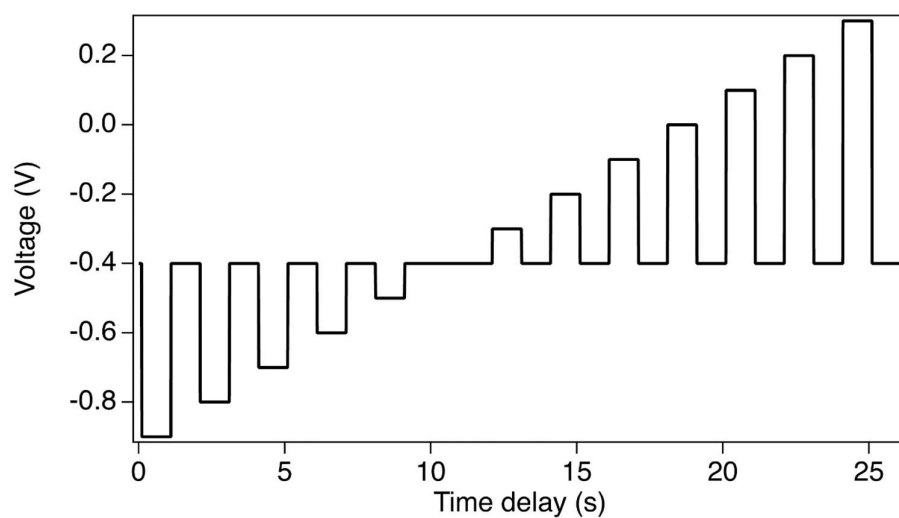


\*\*\*\*\*SUPPORTING INFORMATION\*\*\*\*\*

**Synergistic Effects in Ambipolar Blends of Mixed Ionic-Electronic Conductors**

*Eyal Stein, Sasha Simotko, Yogesh Yadav, Priscila Cavassin, Iain McCulloch, Natalie Banerji, Gitti L. Frey\**



**Figure S1.** Profile of the potential steps applied in the films.

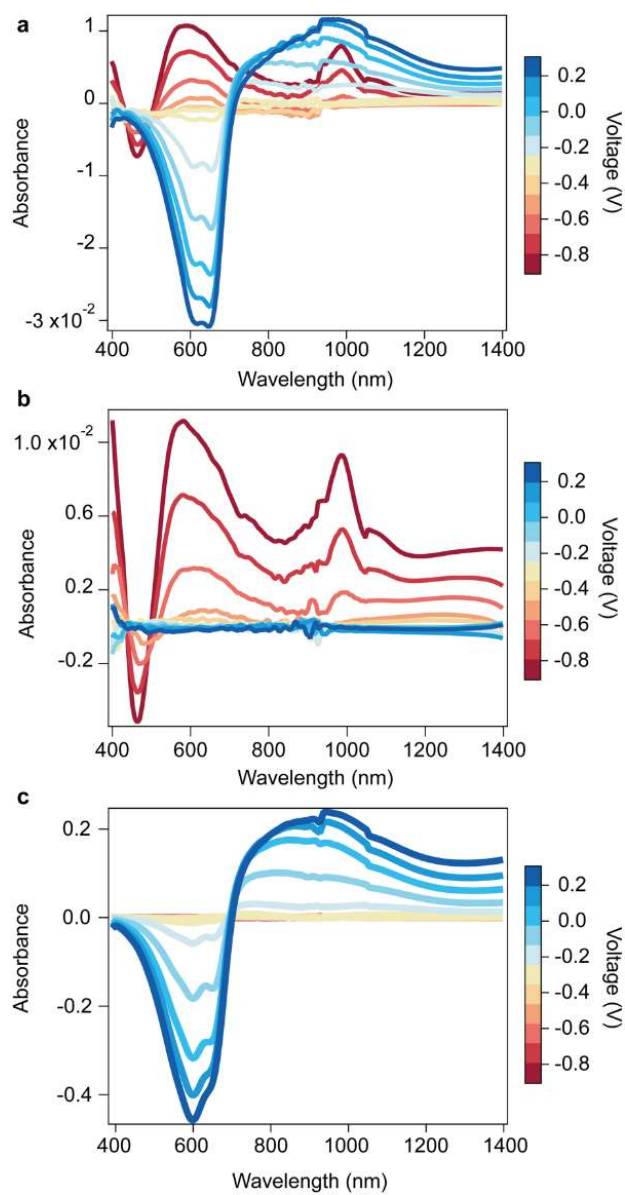


**Figure S2.** Differential steady-state absorbance of 60 nm a) blend 95:5 small molecule: polymer, b) pristine n-type and c) pristine p-type films (with the -0.4 V spectrum subtracted).

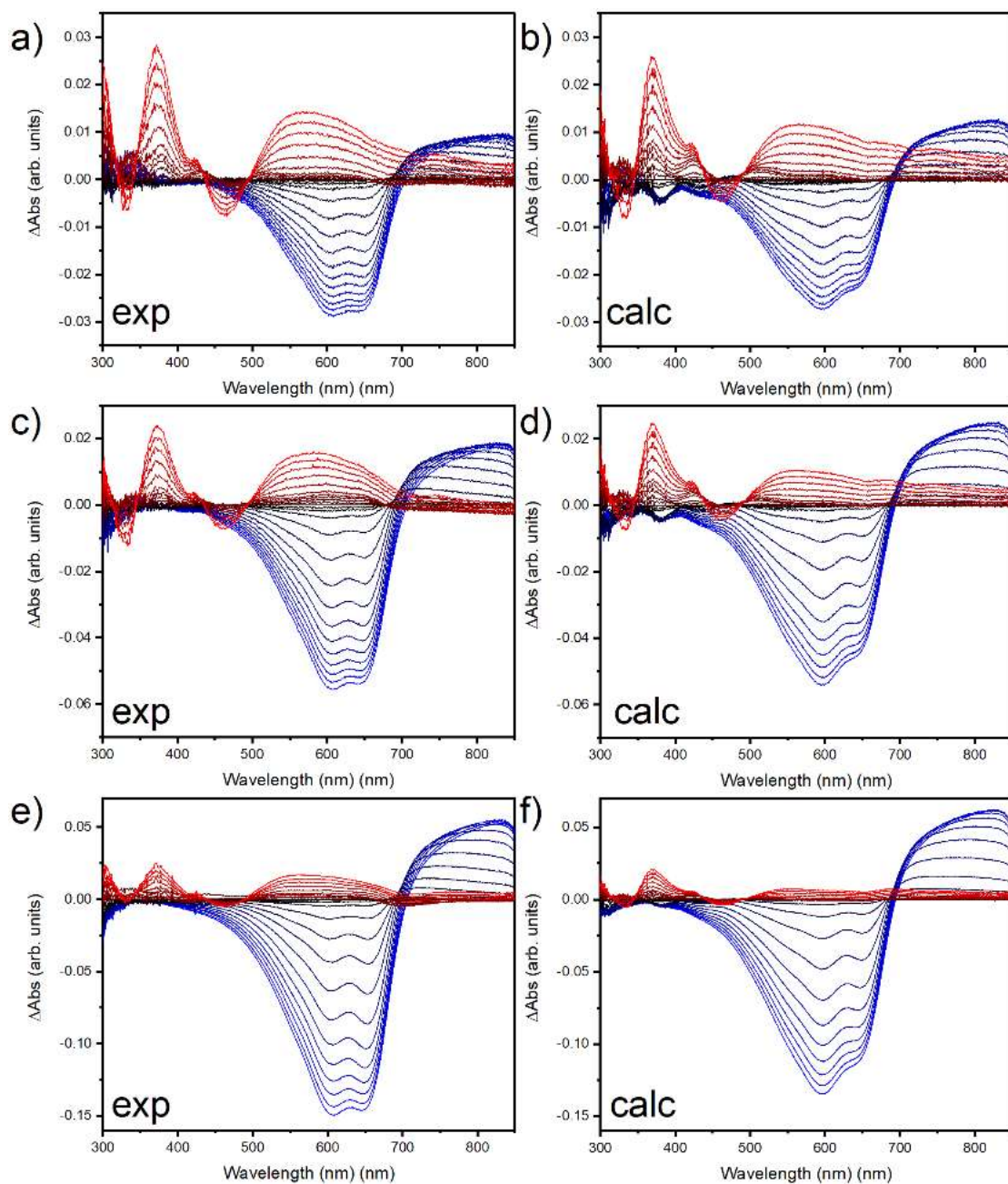


**Figure S3.** Experimental (a,c,e) and rule-of-mixtures calculated (b,d,f) differential absorbance spectra of 5:95, 10:90 and 25:75 p(g2T-TT):PrC<sub>60</sub>MA blends, respectively, applied between +0.3V and -0.9V vs Ag/AgCl and presented with respect to the recorded spectra at  $V_{WE} = -0.4V$ . The experimental figures show an increase in intensity of the 460nm valley and the 560nm peak with respect to their calculated counterparts. Pristine samples results are shown in our previous work (*E. Stein, O. Nahor, M. Stolov, V. Freger, I. M. Petruta, I. McCulloch and G. L. Frey, Nat Commun, 2022, 13, 5548*). Rule of mixtures calculations was performed according to Equation:

$$AbS_{calc} = X_{PrC_{60}MA} \cdot Abs_{PrC_{60}MA} + X_{p(g2T-TT)} \cdot Abs_{p(g2T-TT)}$$

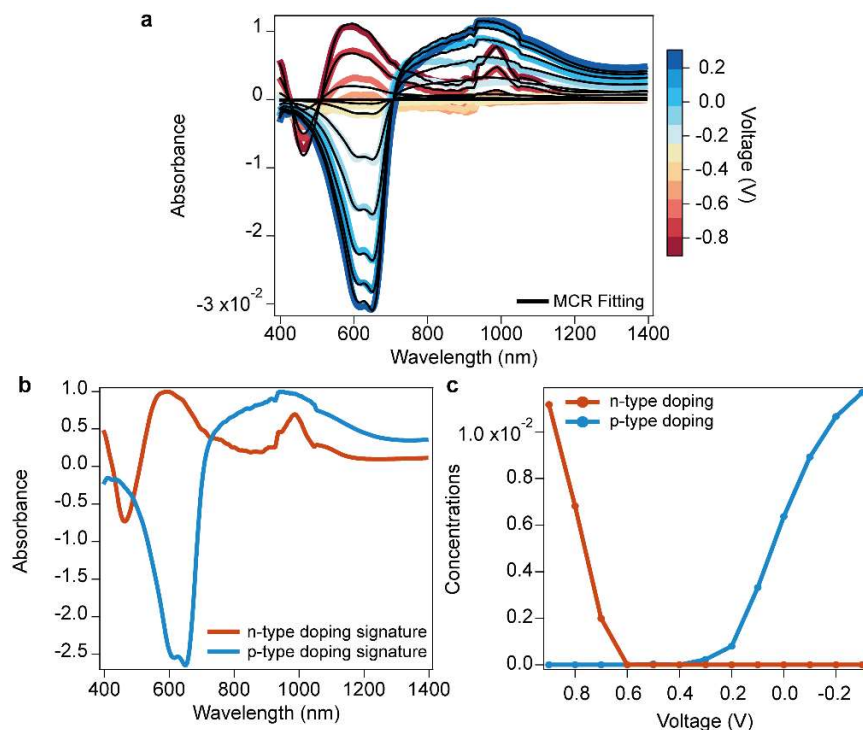


**Figure S4.** a) Steady-state absorbance and MCR fitting of the 60 nm 5:95 blend film, b) spectral signatures obtained with MCR and c) their respective concentrations.

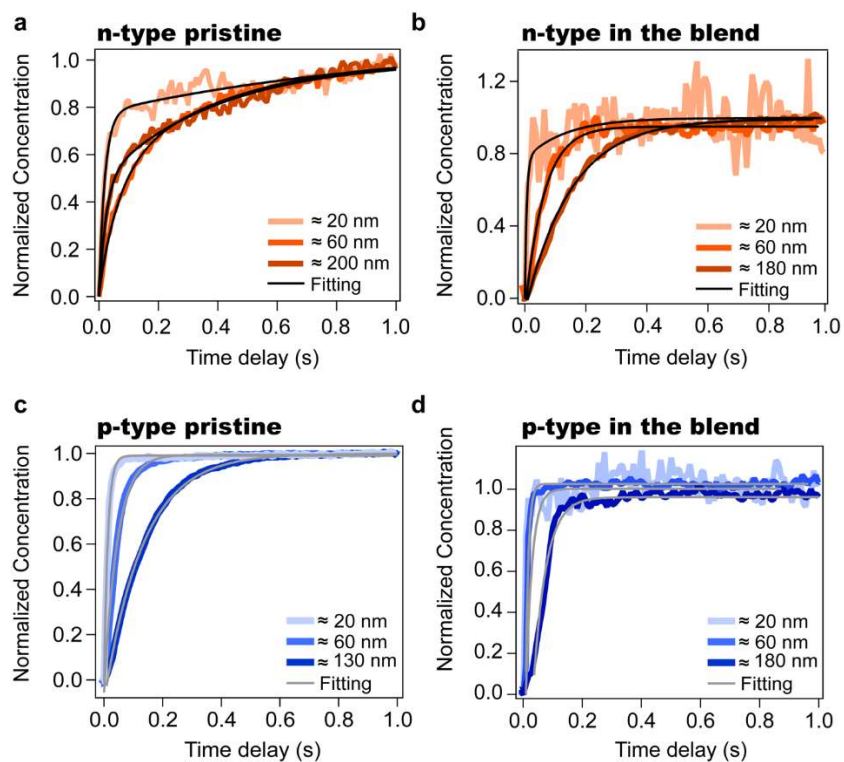


**Figure S5.** Optical doping kinetics of a) n-type pristine films and b) n-type in the 5:95 blend while applying a voltage step from -0.4 to -0.9 V. c) doping kinetics of pristine p-type films and d) p-type in 5:95 blend while applying a voltage step from -0.4 V to +0.3 V. The multi-exponential fits are shown in grey. The concentrations of the charges were obtained from MCR decomposition of the spectroelectrochemistry data and normalized.

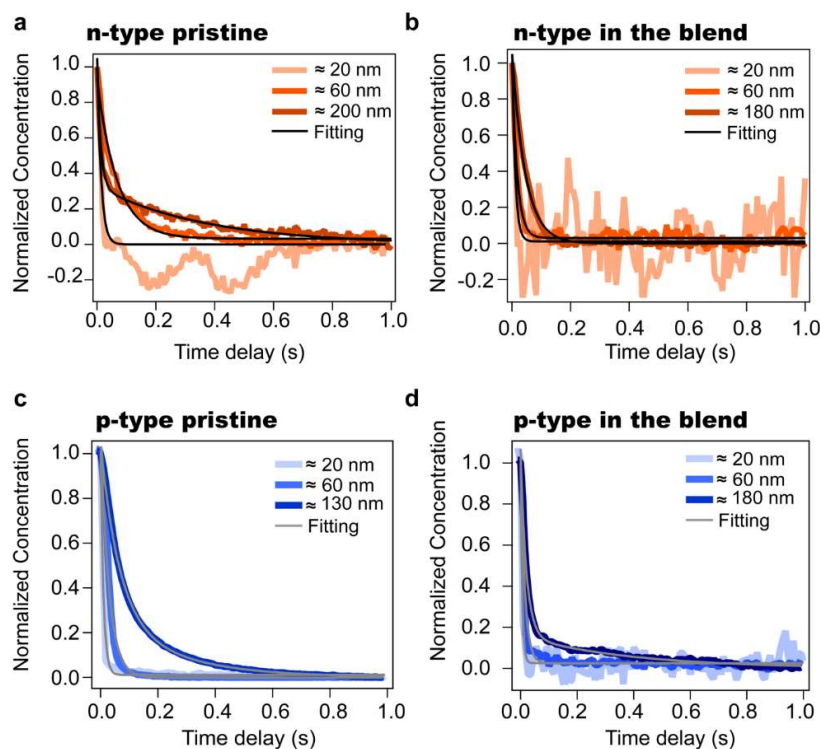


**Figure S6.** Optical dedoping kinetics of a) n-type pristine films and b) n-type in the 5:95 blend while applying a voltage step from -0.9 to -0.4 V. c) doping kinetics of pristine p-type films and d) p-type in 5:95 blend while applying a voltage step from 0.3 V to -0.4 V. The multi-exponential fits are shown in grey. The concentrations of the charges were obtained after MCR decomposition and normalized.

The normalized concentrations during doping/dedoping were fit with the following biexponential equation:

$$C(t) = A_1 \exp\left(-\frac{t}{\tau_1}\right) + A_2 \exp\left(-\frac{t}{\tau_2}\right) + y$$

**Table S1.** Fitting parameters during optical doping.

	<i>p-type pristine</i>			<i>n-type pristine</i>		
	20 nm	60 nm	130 nm	20 nm	60 nm	200 nm
$\tau_1(s)$	<b>0.01</b> (100%)	<b>0.04</b> (100%)	<b>0.13</b> (100%)	<b>0.01</b> (72%)	<b>0.07</b> (49%)	<b>0.02</b> (49%)
$\tau_2(s)$	-	-	-	<b>1.01</b> (28%)	<b>0.40</b> (51%)	<b>0.40</b> (51%)
$y$	<b>0.99</b> (100%)	<b>0.99</b> (100%)	<b>1.00</b> (100%)	<b>1.07</b> (100%)	<b>1.01</b> (100%)	<b>1.00</b> (100%)
	<i>p-type blend</i>			<i>n-type blend</i>		
	20 nm	60 nm	180 nm	20 nm	60 nm	180 nm
$\tau_1(s)$	<b>0.01</b> (100%)	<b>0.02</b> (100%)	<b>0.04</b> (100%)	<b>0.01</b> (77%)	<b>0.06</b> (100%)	<b>0.15</b> (100%)
$\tau_2(s)$	-	-	-	<b>0.13</b> (23%)	-	-
$y$	<b>1.02</b> (100%)	<b>1.03</b> (100%)	<b>1.01</b> (100%)	<b>1.00</b> (100%)	<b>0.95</b> (100%)	<b>0.99</b> (100%)

**Table S2.** Fitting parameters during optical dedoping.

	<i>p-type pristine</i>			<i>n-type pristine</i>		
	20 nm	60 nm	130 nm	20 nm	60 nm	200 nm
$\tau_1$ (s)	<b>0.01</b> (99%)	<b>0.03</b> (100%)	<b>0.06</b> (73%)	<b>0.01</b> (100%)	<b>0.07</b> (97%)	<b>0.01</b> (67%)
$\tau_2$ (s)	-	-	<b>0.24</b> (27%)	-	-	<b>0.37</b> (33%)
$\gamma$	<b>0.01</b> (1%)	<b>0.00</b> (0%)	<b>0.00</b> (0%)	<b>0.00</b> (0%)	<b>0.03</b> (3%)	<b>0.00</b> (0%)
	<i>p-type blend</i>			<i>n-type blend</i>		
	20 nm	60 nm	180 nm	20 nm	60 nm	180 nm
$\tau_1$ (s)	<b>0.01</b> (97%)	<b>0.01</b> (97%)	<b>0.02</b> (85%)	<b>0.01</b> (99%)	<b>0.02</b> (96%)	<b>0.05</b> (100%)
$\tau_2$ (s)	-	-	<b>0.39</b> (15%)	-	-	-
$\gamma$	<b>0.03</b> (3%)	<b>0.02</b> (3%)	<b>0.00</b> (0%)	<b>0.01</b> (1%)	<b>0.03</b> (4%)	<b>0.00</b> (0%)

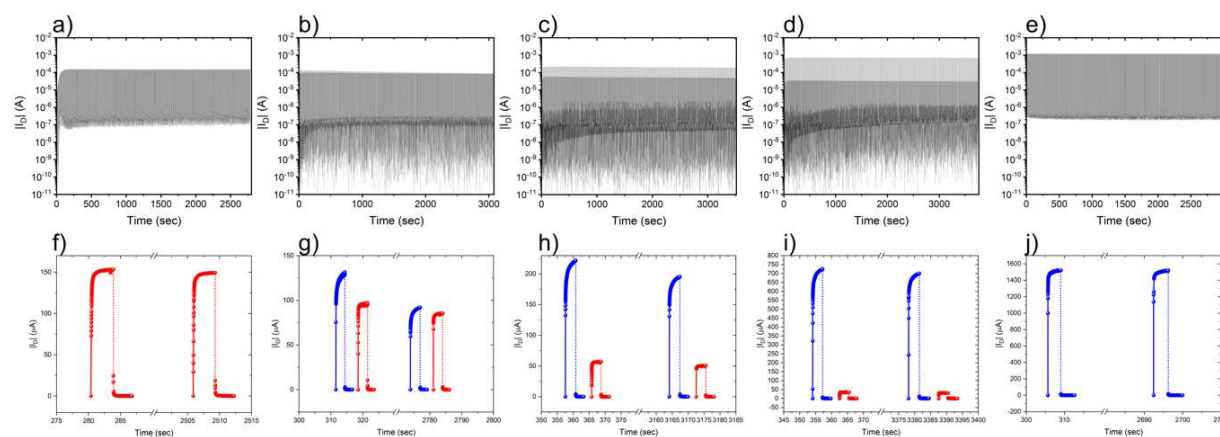


**Figure S7.** Stability measurements of a single typical device for each blend composition. a)-e) 400 ON-OFF cycles and f)-j) an inset of the 40th and 360th cycles for response time and degradation calculation of compositions 0:100, 5:95, 10:90, 25:75, 100:0 p(g2T-TT):PrC<sub>60</sub>MA respectively.

**Table S3.** The turn-on and turn-off potentials applied to keep the same driving force in the electrical transient measurements,  $|V_{th} - V_{OFF}| = 0.1V$ ,  $|V_{th} - V_{ON}| = 0.25V$ .

		$V_{th}$ [V]	$V_{ON}$ [V]	$V_{OFF}$ [V]
p(g2T – TT)	p	0.001	-0.249	0.101
25: 75		-0.037	-0.287	0.063
10: 90		-0.050	-0.300	0.050
5: 95		-0.076	-0.326	0.024
PrC <sub>60</sub> MA				
p(g2T – TT)	n			
25: 75		0.621	0.521	0.871
10: 90		0.617	0.517	0.867
5: 95		0.610	0.510	0.860
PrC <sub>60</sub> MA		0.620	0.520	0.870

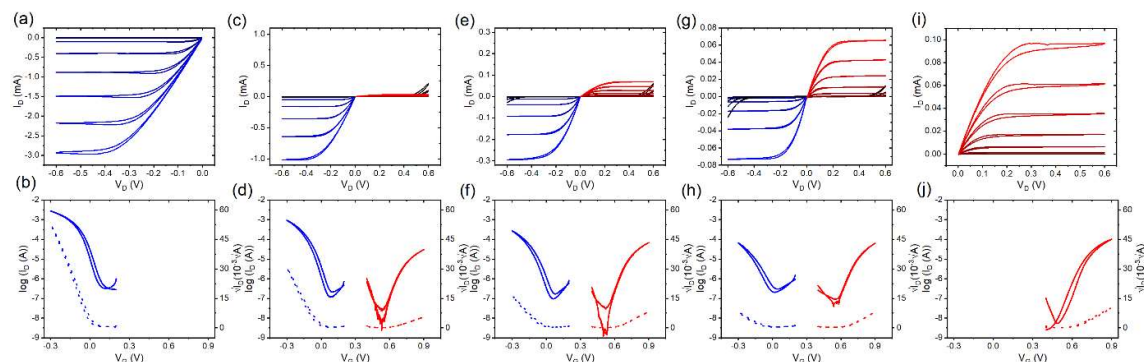


**Figure S8.** Organic Electrochemical Transistors for various blend compositions: a)-b) p(g2T-TT), c)-d) 25:75, e)-f) 10:90, g)-h) 5:95, i)-j) PrC<sub>60</sub>MA. Partially adopted from *E. Stein, O. Nahor, M. Stolov, V. Freger, I. M. Petruta, I. McCulloch and G. L. Frey, Nat Commun, 2022, 13, 5548*. In the output curves,  $\Delta V_G = 0.05V$  between each curve. In the transfer curves  $V_D = \pm 0.4V$  for n- and p-type respectively.

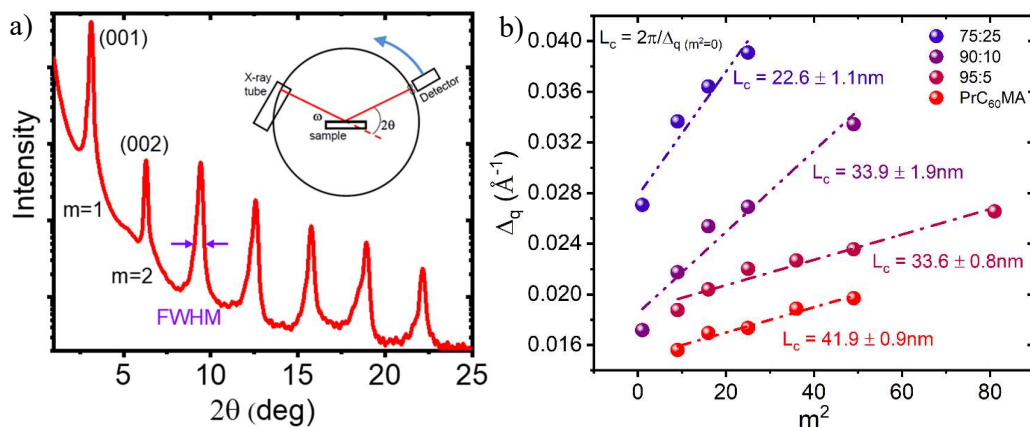


**Figure S9.** Scherrer analysis of the (001) coherence length of PrC<sub>60</sub>MA in various compositions, using a pseudo-voigt function fitting. a) an example PrC<sub>60</sub>MA out-of-plane x-ray diffraction that shows a FWHM and peak orders used for the fitting. b) The complete analysis of  $\Delta_q$  (FWHM) vs square peak order ( $m^2$ ) with linear regression and the resulting coherence length. Partially reproduced from *E. Stein, O. Nahor, M. Stolov, V. Freger, I. M. Petruta, I. McCulloch and G. L. Frey, Nat Commun, 2022, 13, 5548*.

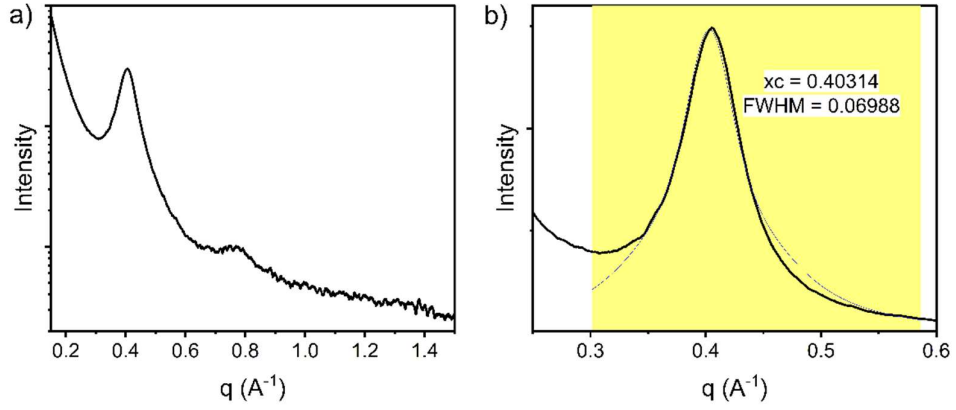


**Figure S10.** a) 1D-XRD measurement of p(g2T-TT), and b) its FWHM according to a pseudo-voigt fitting curve yielding  $\Delta_q = 0.06988[\text{Å}^{-1}]$  and therefore  $L_c = \frac{2\pi K}{\Delta_q} \sim 8\text{nm}$  for  $K = 0.9$ .

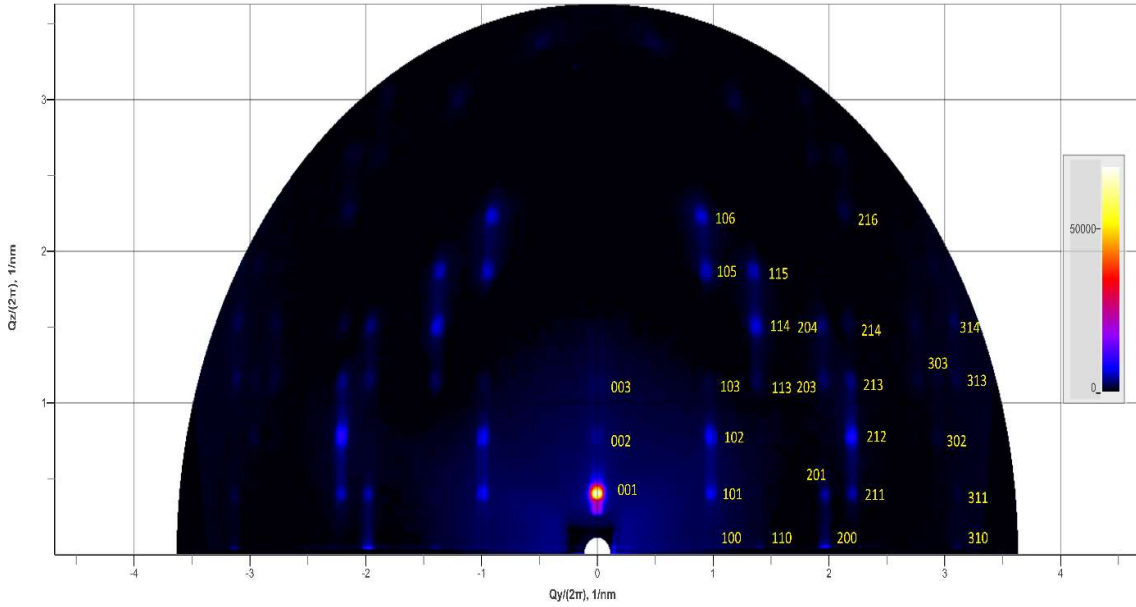


**Figure S11.** GIWAXS pattern of pristine PrC<sub>60</sub>MA assigned with (hkl) miller indices fit for a tetragonal crystalline structure with calculated lattice parameters  $a = b \approx 1\text{nm}$ ,  $c \approx 2.5\text{nm}$ .

The calculation of lattice parameters from miller indices under the assumption that the crystal system is Tetragonal goes as follows:

$$\frac{1}{d^2} = \frac{h^2 + k^2}{a^2} + \frac{l^2}{c^2}$$

Where  $d$  is the interplanar spacing,  $a$  and  $c$  are tetragonal lattice parameters and  $h, k, l$  are the miller indices. The interplanar spacings are calculated using the known relationship  $d = \frac{2\pi}{q}$  where  $q$  is the wave vector and is extracted from the GIWAXS pattern on the detector.

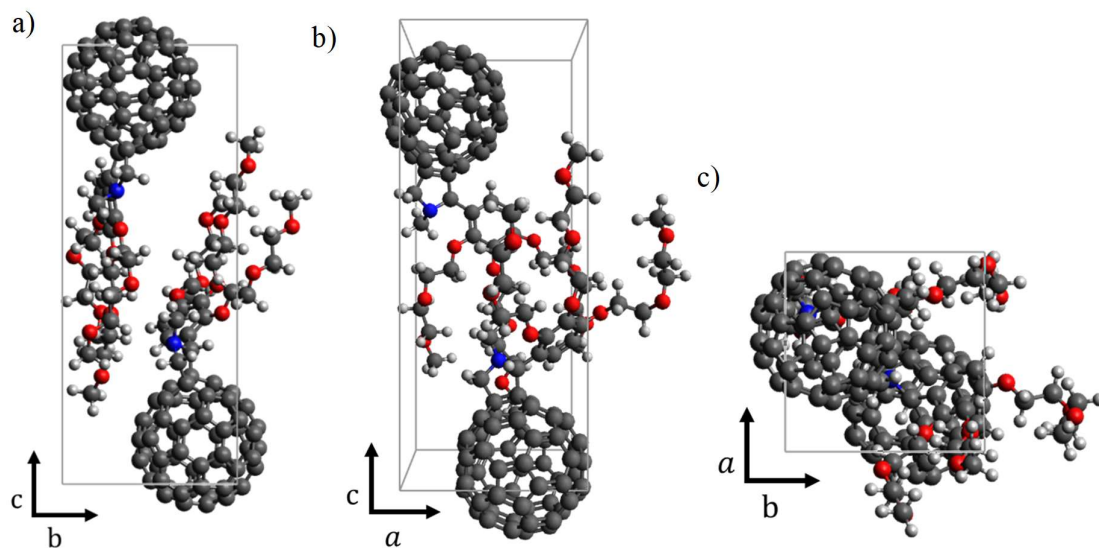


**Figure S12.** Approximated simulation of the PrC<sub>60</sub>MA tetragonal unit cell in the a) yz, b) xz and c) xy plane.

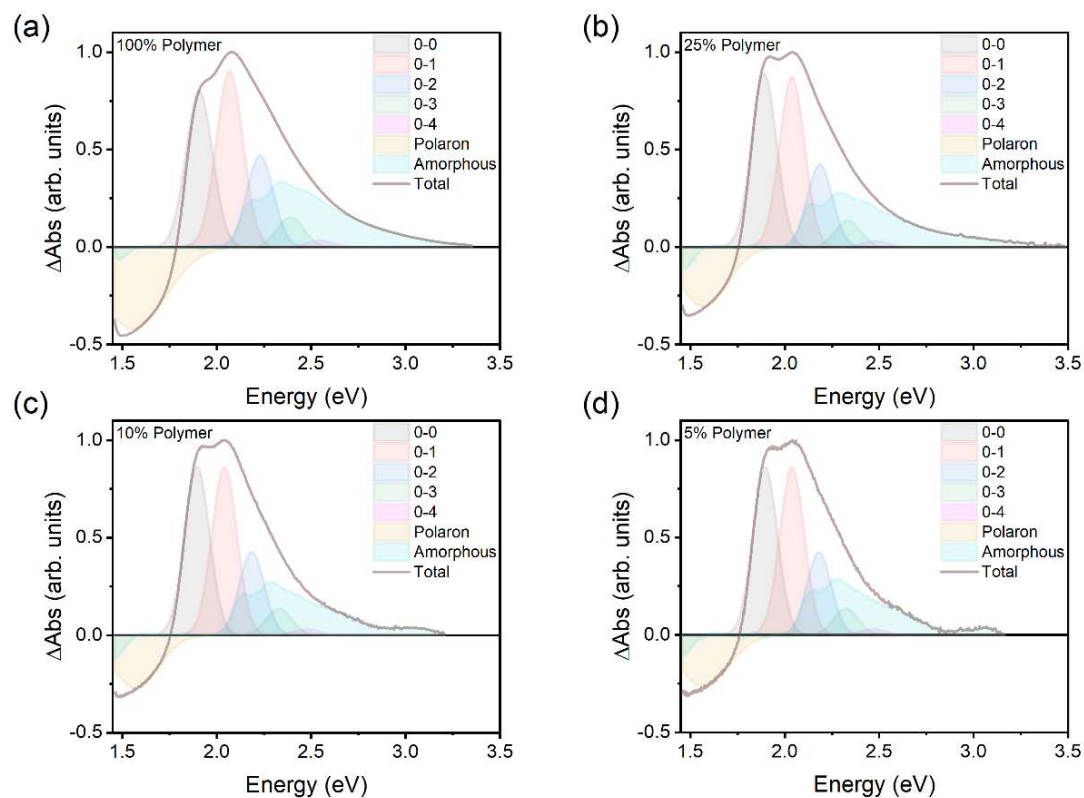


**Figure S13.** Normalized differential absorbance spectra of a) p(g2T-TT) and its blends (b-d) with model fitting according to FC Spano's H-aggregate absorption model. The fitting was performed for 5 vibronic components (0-0, 0-1...0-4) and a single polaronic component.

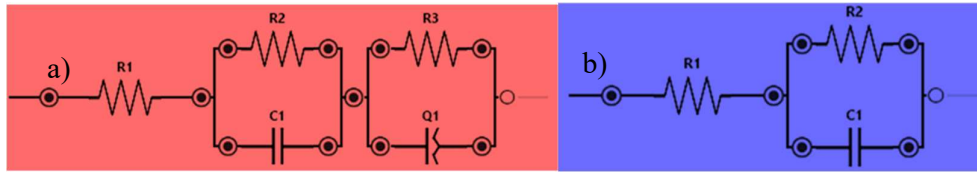


**Figure S14.** The circuits used in the fitting of EIS results for the a) n-type behavior as a semi-ideal voigt circuit and the b) p-type behavior as a simplified randles circuit.

**Table S4.** Fitting parameters of EIS results at +0.3V for p-type doping and -0.9V for n-type doping. Each composition has 2 pixels measured, therefore 2 columns of results for pixel 1 (left) and pixel 2 (right).

	PrC <sub>60</sub> MA		5:95				10:90				25:75				p(g2T-TT)	
	n-type		n-type		p-type		n-type		p-type		n-type		p-type		p-type	
R1 (Ω)	556	552	424	432	706	680	502	492	650	634	514	581	770	820	532	520
R2 (MΩ)	1.68	1.80	0.99	1.73	18.4	21.1	1.23	1.24	20.1	26.2	2.16	3.41	17.3	17.7	13.1	11.5
C1 (μF)	1.28	1.39	2.21	2.52	0.30	0.40	1.15	1.26	0.32	0.34	1.39	1.35	0.93	0.91	4.09	3.64
R3 (kΩ)	5.34	6.09	44.5	32.0	-	-	7.52	7.99	-	-	8.99	11.4	-	-	-	-
Q1 (μT)	7.10	4.73	0.16	0.11	-	-	4.08	4.18	-	-	2.64	2.06	-	-	-	-
n1 (φ)	0.55	0.59	0.46	0.50	-	-	0.58	0.59	-	-	0.61	0.63	-	-	-	-
χ <sup>2</sup>	0.002	0.005	0.006	0.003	0.168	0.137	0.005	0.004	0.040	0.028	0.003	0.004	0.059	0.091	0.004	0.004

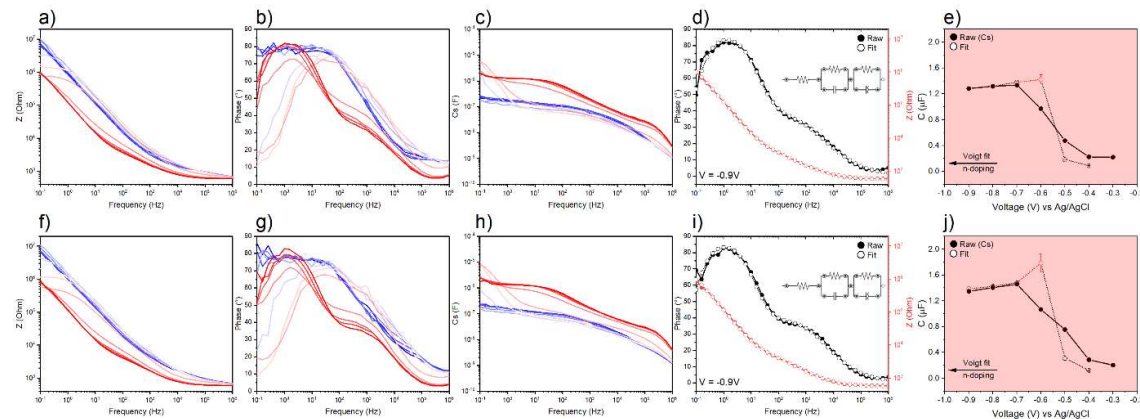


**Figure S15.** EIS results of PrC<sub>60</sub>MA film in 0.1 M KCl aqueous electrolyte from +0.3V to -0.9V (max n-doping) and fit to both voigt cell  $R(RC)(RQ)$  and  $Cs = \frac{1}{2\pi fZ''}$  at 1Hz. a-e) EIS pad 1, f-j) EIS pad 2.

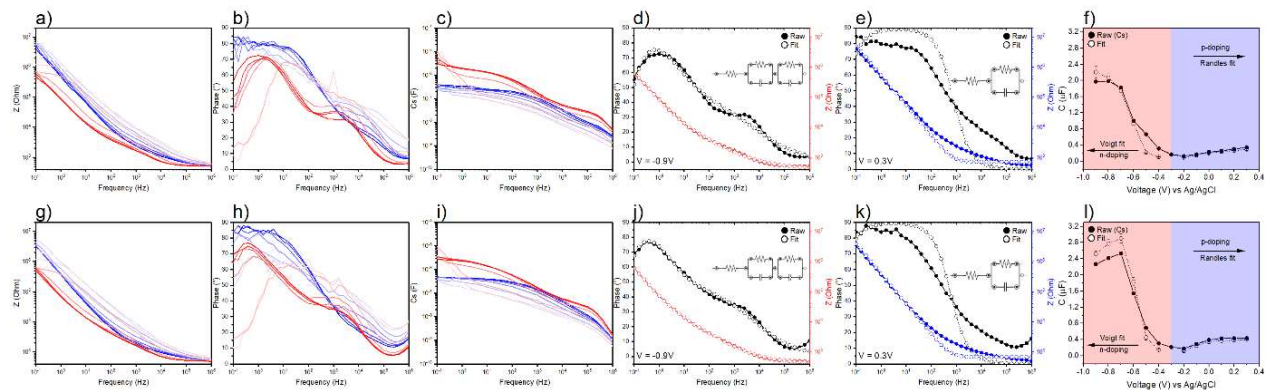


**Figure S16.** EIS results of p(g2T-TT):PrC<sub>60</sub>MA 5:95 blend film in 0.1 M KCl aqueous electrolyte from +0.3V (max p-doping) to -0.9V (max n-doping) and fit to both randles cell  $R(RC)$  and  $Cs = \frac{1}{2\pi fZ''}$  at 1Hz. a-f) EIS pad 1, g-l) EIS pad 2.

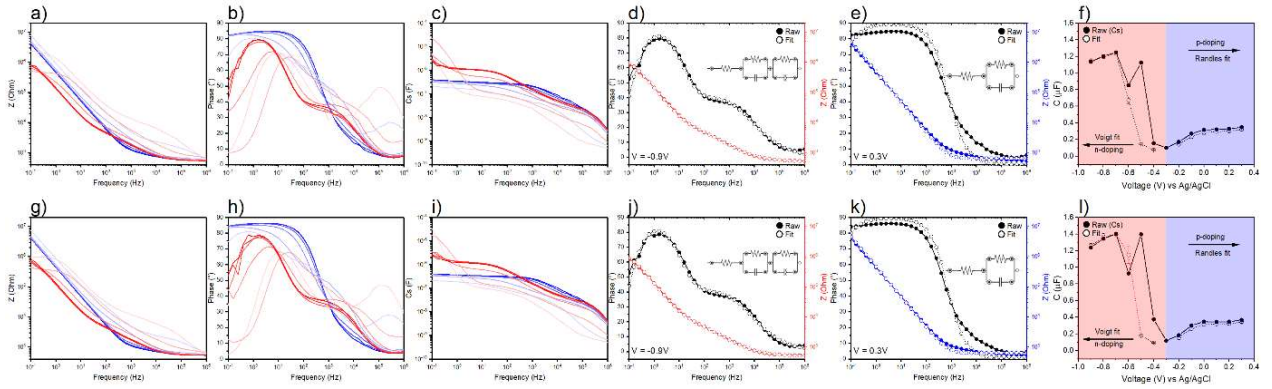


**Figure S17.** EIS results of p(g2T-TT):PrC<sub>60</sub>MA 10:90 blend film in 0.1 M KCl aqueous electrolyte from +0.3V (max p-doping) to -0.9V (max n-doping) and fit to both randles cell R(RC) and  $C_s = \frac{1}{2\pi fZ''}$  at 1Hz. a-f) EIS pad 1, g-l) EIS pad 2.

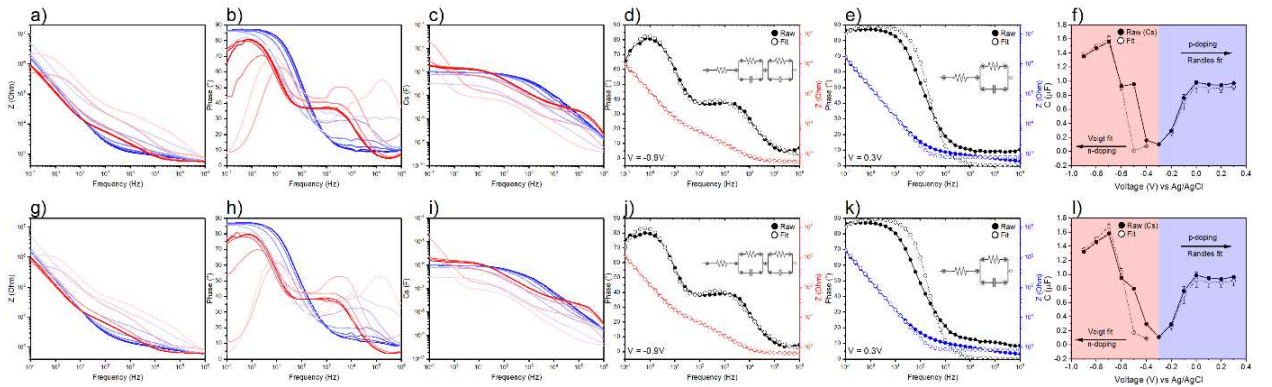


**Figure S18.** EIS results of p(g2T-TT):PrC<sub>60</sub>MA 25:75 blend film in 0.1 M KCl aqueous electrolyte from +0.3V (max p-doping) to -0.9V (max n-doping) and fit to both randles cell R(RC) and  $C_s = \frac{1}{2\pi fZ''}$  at 1Hz. a-f) EIS pad 1, g-l) EIS pad 2.

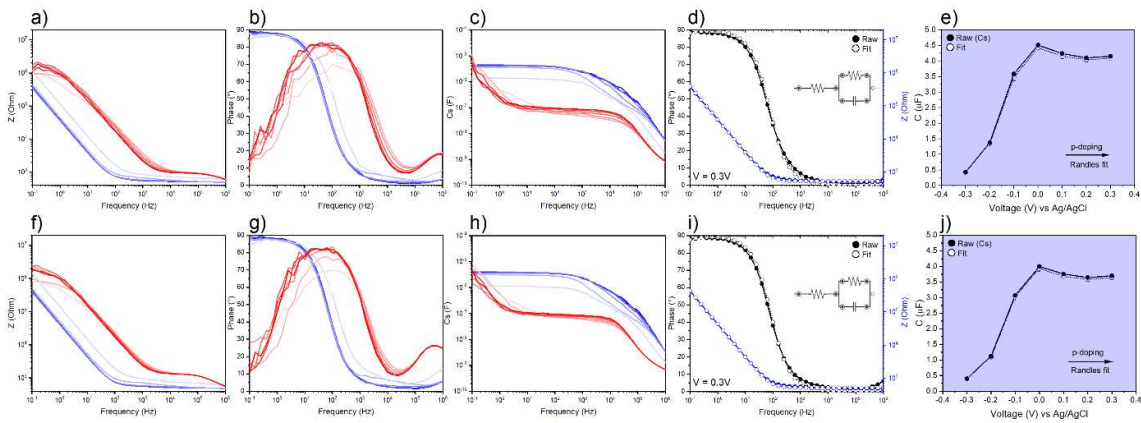


**Figure S19.** EIS results of p(g2T-TT) film in 0.1 M KCl aqueous electrolyte from +0.3V (max p-doping) to -0.9V and fit to both randles cell R(RC) and  $C_s = \frac{1}{2\pi fZ''}$  at 1Hz. a-e) EIS pad 1, f-j) EIS pad 2.

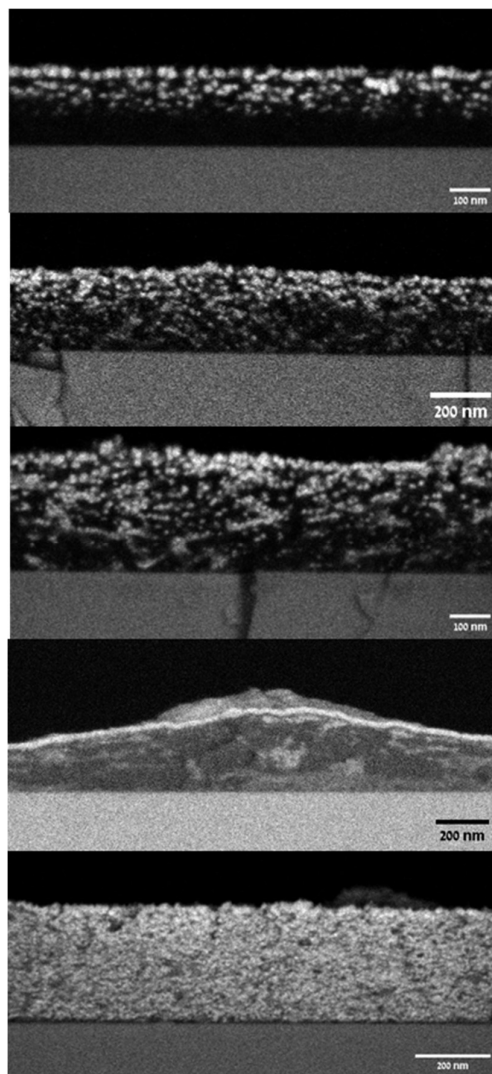


**Figure S20.** Cross-sectional HRSEM micrographs of ZnO Vapor Phase Infiltrated films taken in a Backscattered electrons detector. From top to bottom: PrC<sub>60</sub>MA, 5:95, 10:90, 25:75, p(g2T-TT). White regions are ZnO and dark regions are organic matter, the substrate is Silicon. Black area above the samples is vacuum.

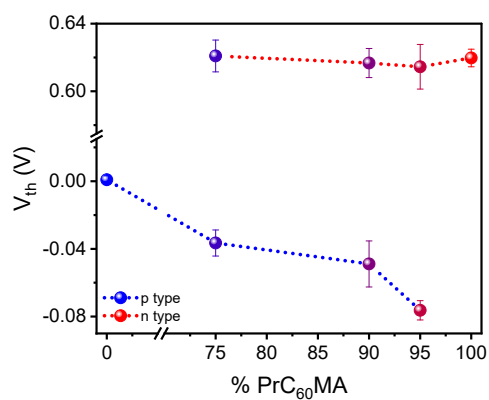


**Figure S21.** Calculated threshold voltage for various blend compositions and pristine materials.